eScience 3 (2023) 100093

Contents lists available at ScienceDirect

eScience

journal homepage: www.keaipublishing.com/en/journals/escience

Perspective

Anode corrosion in aqueous Zn metal batteries

Zhao Cai [a,b,1], Jindi Wang [a,c,1], Yongming Sun [a,*]

[a] *Wuhan National Laboratory for Optoelectronics, Huazhong University of Science and Technology, Wuhan 430074, China*
[b] *Faculty of Materials Science and Chemistry, China University of Geosciences (Wuhan), Wuhan 430074, China*
[c] *Institute of New Energy on Chemical Storage and Power Sources, College of Applied Chemistry and Environmental Engineering, Yancheng Teachers University, Yancheng 224000, China*

HIGHLIGHTS

- The development of aqueous Zn batteries, from the first voltaic pile to very recent sustainable Zn batteries, is summarized.
- The corrosion mechanisms of aqueous Zn anodes in both alkaline and neutral electrolytes are discussed.
- Potential future research directions are proposed for next-generation aqueous Zn anode materials.

GRAPHICAL ABSTRACT

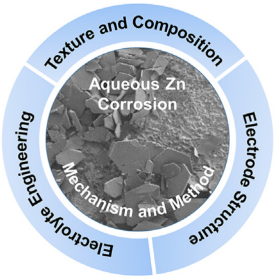

ARTICLE INFO

Keywords:
Aqueous batteries
Zn metal anode
Chemical oxidation
Electrochemical hydrogen evolution
Corrosion mechanism
Surface protection

ABSTRACT

Given their low cost and intrinsic safety, aqueous Zn metal batteries (AZMBs) are drawing increasing attention in the field of smart grids and large-scale energy storage. However, the Zn metal anode in aqueous electrolyte suffers from a critical issue, corrosion, which must be fully addressed before the practical implementation of AZMBs. In this perspective, the mechanisms of aqueous Zn metal anode corrosion in both alkaline and neutral electrolytes are compared and discussed. The methods for studying the corrosion processes and the strategies for Zn corrosion protection in AZMBs are also summarized. Finally, some expectations about potential research directions for making corrosion-resistant AZMBs a commercial reality are provided.

1. Introduction

With the rapid growth of global economies, energy demands worldwide are becoming much more pressing, stimulating a burgeoning research interest in grid energy storage technologies [1–6]. A number of advantages make aqueous batteries employing Zn metal anodes highly promising for large-scale energy storage, including 1) high theoretical capacities of 820 mAh g^{-1} and 5854 mAh cm^{-3} for metallic Zn [7]; 2) the low electrode potential of Zn^{2+}/Zn^0 (−0.76 V vs. reversible hydrogen electrode) [8]; and 3) the low cost and high safety of both metallic Zn and aqueous electrolytes [9].

The AZMB is not a fresh concept; it is, in fact, a century-old technology [10–12]. The first aqueous Zn battery, the voltaic pile, was invented by A. Volta in 1799 (Fig. 1a) [13], and T. A. Edison developed an alkaline Ni–Zn battery system in 1901 [14]. However, alkaline Zn batteries generally scuffer from Zn dendrite issues at the anode, leading to short battery life span [15,16]. To tackle these issues in alkaline Zn chemistry, Yamamoto and co-workers investigated Zn battery systems with mild aqueous $ZnSO_4$

---

* Corresponding author.
E-mail address: yongmingsun@hust.edu.cn (Y. Sun).
[1] These authors contributed equally to this work.

https://doi.org/10.1016/j.esci.2023.100093
Received 1 September 2022; Received in revised form 28 November 2022; Accepted 4 January 2023
Available online 11 January 2023

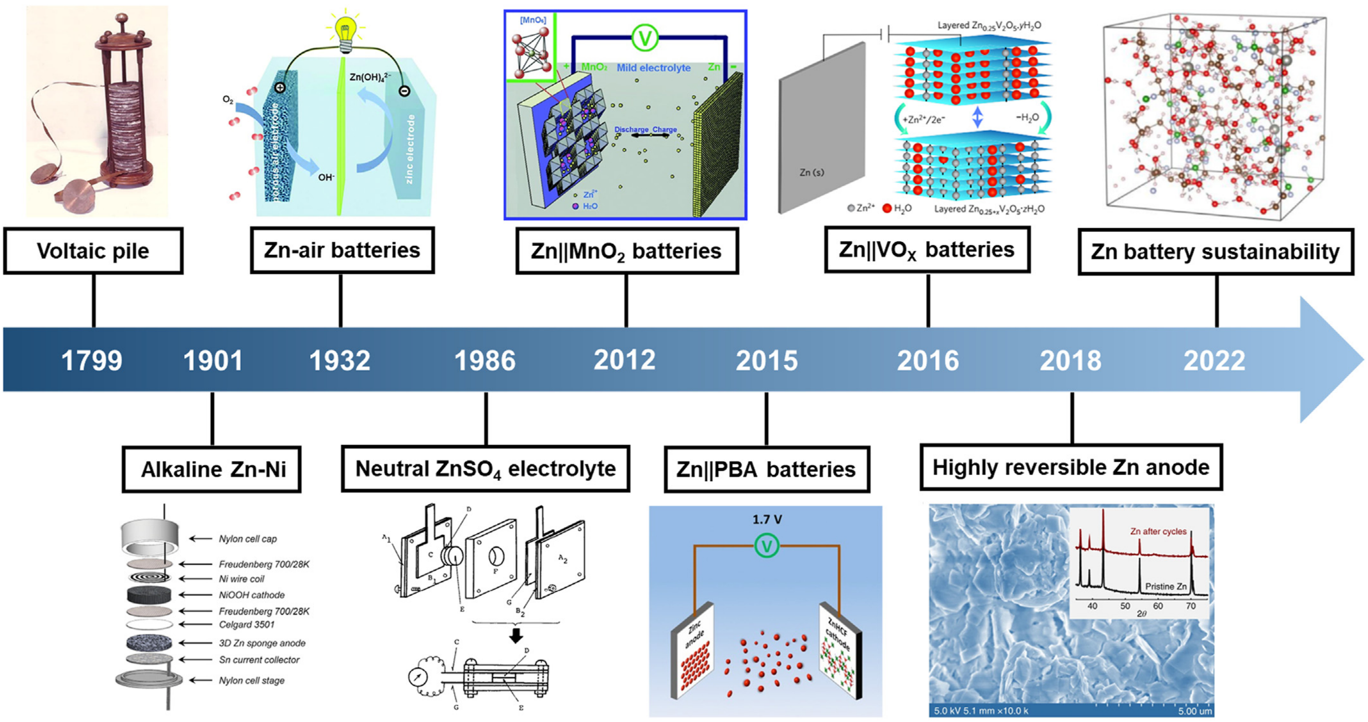

Fig. 1. A timeline demonstrating the development of AZMBs. Reproduced with permission from Ref. [13], copyright 2011 Springer Nature. Reproduced with permission from Ref. [23], copyright 2017 American Association for the Advancement of Science. Reproduced with permission from Ref. [24], copyright 2014 Royal Society of Chemistry. Reproduced with permission from Ref. [17], copyright 1986 Elsevier. Reproduced with permission from Ref. [25], copyright 2012 Wiley-VCH. Reproduced with permission from Ref. [20], copyright 2015 Wiley-VCH. Reproduced with permission from Ref. [26], copyright 2016 Springer Nature. Reproduced with permission from Ref. [21], copyright 2018 Springer Nature. Reproduced with permission from Ref. [22], copyright 2022 Springer Nature.

electrolyte, which yielded improved reversibility in aqueous Zn anodes and batteries [17]. Since then, extensive efforts have been devoted to developing novel Zn battery systems with neutral/mild acidic electrolytes, such as Zn||MnO_2 [18], Zn||VO_x [19], and Zn||Prussian blue analogues (PBAs) batteries [20]. Notably, Wang et al., in 2018 proposed a highly reversible Zn electrode using concentrated electrolyte [21]. Yang et al. very recently have designed a non-flammable $Zn(BF_4)_2$/ethylene glycol hydrous-organic electrolyte for sustainable Zn batteries [22], attracting much research interest to the field of aqueous Zn anodes. Yet despite these exciting achievements, designing and fabricating high-performance Zn anodes for practical AZMBs remains a great challenge.

Due to the high chemical activity and low electrochemical potential of metallic Zn, corrosion is spontaneous in an aqueous Zn system [27–31], as exemplified by the chemical Zn oxidation [32] and electrochemical hydrogen evolution side-reactions [33]. In alkaline Zn chemistry, the corrosion of aqueous Zn anodes produces amphoteric ZnO and hydrogen gas [34]. On the other hand, Zn corrosion in neutral/mild acidic electrolytes results in insoluble $Zn(OH)_2$/zinc hydroxide sulfate (ZHS) as well as hydrogen bubbles [35]. These facts are of vital importance for anode performance optimization and require particular attention. In this perspective, the chemical and electrochemical corrosion phenomena and mechanisms of aqueous Zn anodes are clarified. The methods for understanding Zn corrosion in AZMBs are introduced, and the current strategies for corrosion protection are also discussed. Finally, the challenges and potential future research directions in the field of next-generation AZMB anodes are presented. We hope this perspective will draw special attention to anode corrosion in AZMBs and facilitate the practical development of AZMBs with long shelf life and cycle life.

2. Corrosion mechanisms of aqueous Zn anodes

Zn corrosion in aqueous batteries is generally divided into two classes: one is chemical oxidation corrosion [36,37], which takes place at the Zn surface accessible to the aqueous electrolyte, whether or not the AZMB is in a resting or cycling state; the other is electrochemical hydrogen evolution corrosion [38,39], whereby protons or water molecules accept electrons on the anode surface and are then reduced to hydrogen during metallic Zn plating or battery charging. For AZMBs in a resting state, chemical oxidation corrosion dominates, since electrochemical hydrogen evolution corrosion cannot be triggered at this stage. When the batteries are electrochemically cycled, electrochemical hydrogen evolution corrosion dominates due to the significantly inhibited chemical oxidation of Zn by repeated Zn plating/stripping reactions.

The corrosion mechanism of aqueous Zn anodes varies according to the pH of the electrolyte. In an alkaline electrolyte (e.g., KOH solution), Zn metal is oxidized by OH^- to produce $Zn(OH)_4{}^{2-}$, which is ultimately converted to ZnO (i.e., $Zn + 4OH^- \rightarrow Zn(OH)_4{}^{2-} + 2e^- \rightarrow ZnO + 2OH^- + H_2O + 2e^-$) [40]. The as-formed ZnO is generally a dense oxide layer that can isolate the metallic Zn and aqueous electrolyte and prevent further Zn oxidation, resulting in passivation rather than continuous corrosion (Fig. 2a) [41]. Moreover, ZnO is a typical amphoteric oxide that dissolves in alkaline electrolytes, so Zn corrosion is not a major issue in alkaline Zn batteries.

However, in neutral/mild acidic electrolytes such as $ZnSO_4$ solution, Zn metal reacts with H_2O and $ZnSO_4$ to form ZHS (i.e., $3Zn + 6H_2O + ZnSO_4 \rightarrow Zn_4(OH)_6SO_4 + 3H_2$, Fig. 2b) [42]. Unlike ZnO, the as-produced ZHS is generally a loose and porous layer that is unable to isolate metallic Zn and aqueous electrolyte, leading to continuous Zn corrosion until the active Zn or electrolyte is exhausted [43].

In terms of electrochemical corrosion via hydrogen evolution, protons are adsorbed on the Zn anode and reduced to hydrogen in mildly acidic electrolytes (i.e., $2H^+ + 2e^- \rightarrow H_2$) [44]. In neutral or alkaline electrolytes, water molecules accept electrons on the Zn anode and are reduced to hydrogen (i.e., $2H_2O + 2e^- \rightarrow H_2 + 2OH^-$) [45]. The overpotential of electrochemical hydrogen evolution for Zn anodes in mildly acidic electrolytes is much lower than in alkaline conditions (Fig. 2c) [46],

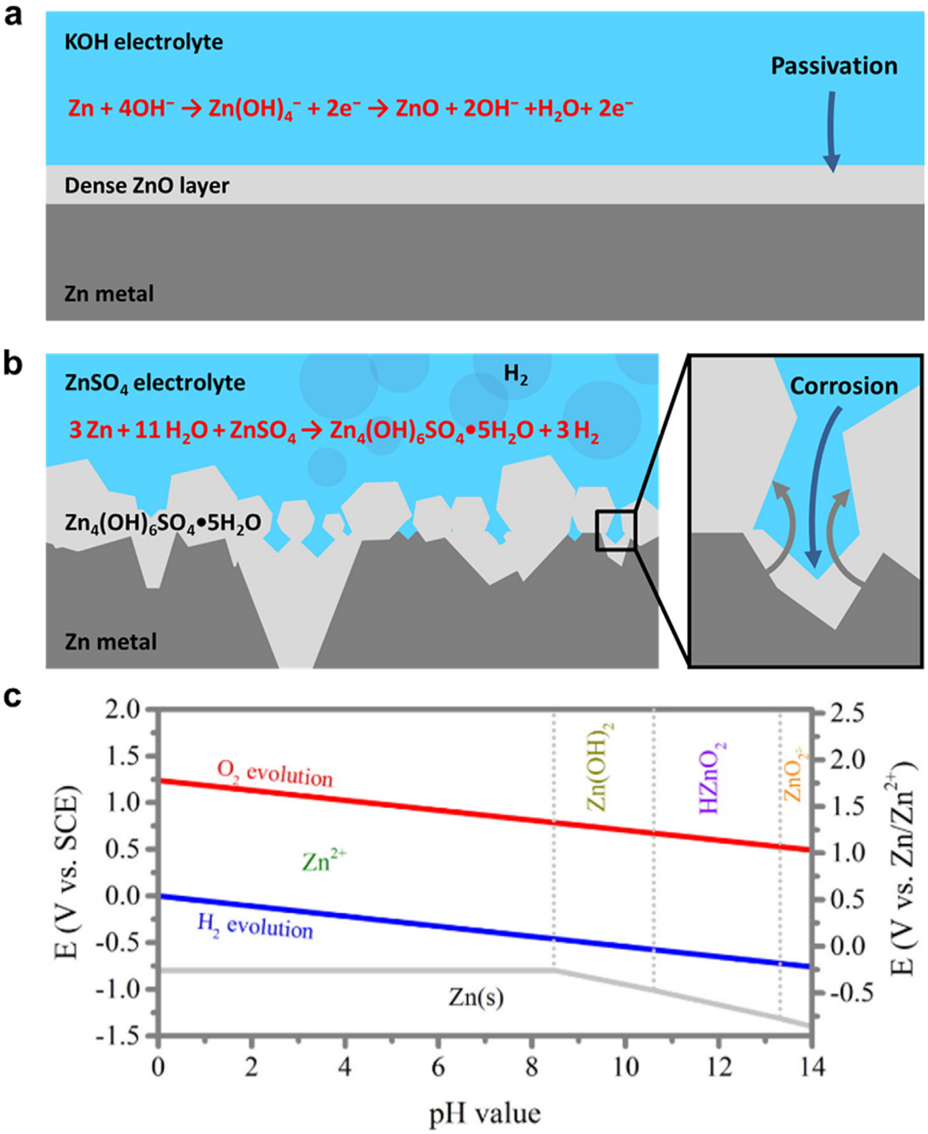

Fig. 2. A schematic showing the chemical oxidation of Zn metal anodes in batteries employing (a) alkaline electrolyte (e.g., KOH) and (b) neutral electrolyte (e.g., $ZnSO_4$). Reproduced with permission from Ref. [36], copyright 2020 Elsevier. (c) Pourbaix diagram of the Zn/H_2O system. Reproduced with permission from Ref. [46], copyright 1974 Wiley-VCH.

which suggests severe electrochemical hydrogen evolution corrosion of the Zn anode will occur in mildly acidic electrolytes such as those based on $ZnSO_4$.

Metallic Zn powders and foils have been widely investigated and adopted as aqueous battery anode materials. Given that Zn powders have a higher specific surface area than Zn foils, the corrosion of Zn powder anodes is more severe in aqueous electrolytes, presenting a major obstacle to the practical application of Zn powder anodes in commercial aqueous batteries [47]. It should also be noted that electrochemical hydrogen evolution corrosion of Zn increases the pH of the micro-environment around the Zn surface [48], promoting the chemical oxidation corrosion of metallic Zn. Thus, both types of corrosion should be analyzed and prevented to achieve corrosion-proof Zn anodes.

3. Methods for Zn corrosion analysis

The black box nature of AZMBs makes it difficult to monitor the Zn corrosion processes inside these sealed systems [49,50]. So far, several methods have been established to analyze Zn corrosion behavior based on two-electrode cells or three-electrode systems; these include electrochemical methods like linear polarization, electrochemical impedance spectroscopy (EIS), Coulombic efficiency (CE), voltage profiles, and non-electrochemical methods like optical microscopy (OM), scanning electron microscopy (SEM), energy dispersive spectroscopy (EDS), X-ray diffraction (XRD), X-ray photoelectron spectroscopy (XPS), *in situ* battery–gas chromatography–mass analysis, etc.

3.1. Electrochemical methods

Linear polarization is one of the most common and reliable methods for investigating Zn corrosion in aqueous electrolytes, as it provides an opportunity to study the corrosion potential (E_{corr}) and corrosion current density (I_{corr}) [51,52]. Fig. 3a demonstrates using linear polarization to analyze the chemical oxidation corrosion of bare Zn and polyamide (PA)-coated Zn with a low scan rate of 1 mV s^{-1} [53]. The E_{corr} located in the open circuit for PA-coated Zn was 20 mV higher than bare Zn, while the I_{corr} obtained by Tafel fitting indicated a lower corrosion rate for PA-coated Zn than bare Zn, suggesting the coated Zn had enhanced chemical corrosion resistance. Fig. 3b presents the use of linear polarization to study the electrochemical hydrogen evolution corrosion of an

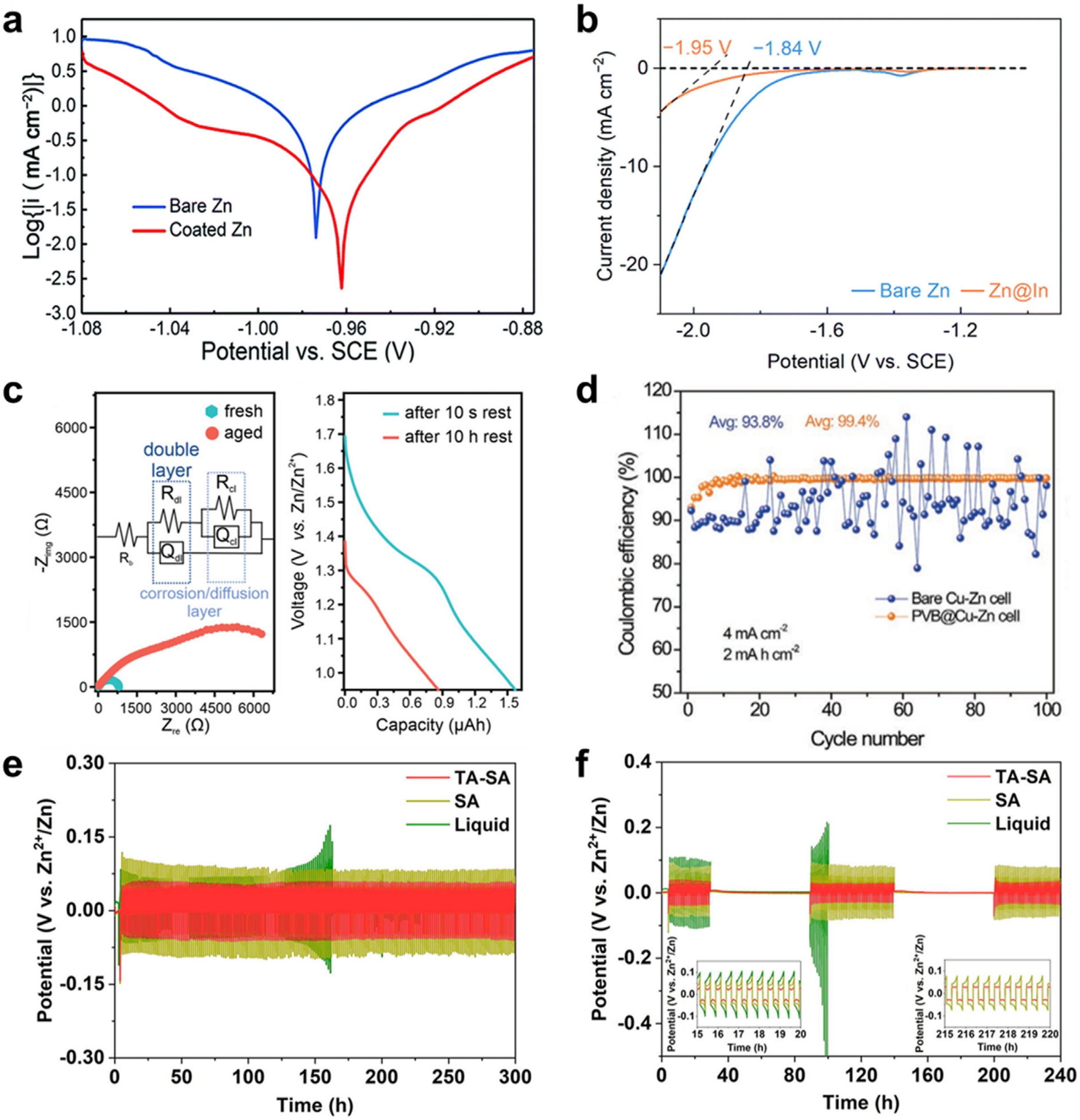

Fig. 3. Linear polarization analysis of (a) chemical corrosion of bare Zn and PA-coated Zn in $ZnSO_4$ electrolyte, and (b) electrochemical hydrogen evolution corrosion of bare Zn anode and Zn@In electrode in 1 M Na_2SO_4. Reproduced with permission from Ref. [53], copyright 2019 Royal Society of Chemistry. Reproduced with permission from Ref. [54], copyright 2022 Royal Society of Chemistry. (c) Nyquist plots of fresh and aged Zn electrodes in $ZnSO_4$ electrolyte (left), and the galvanostatic discharge curves of Zn||MnO_2 batteries after 10 s/10 h of rest (right). Reproduced with permission from Ref. [55], copyright 2021 Wiley-VCH. (d) CEs of bare Cu||Zn and PVB@Cu||Zn half-cells at 4 mA cm^{-2}. Reproduced with permission from Ref. [56], copyright 2020 Wiley-VCH. Voltage profiles of Zn||Zn symmetric cells with (e) continuous cycling at 1.13 mA cm^{-2} and (f) cycling at 1.13 mA cm^{-2} for 30 h combined with resting for 60 h. Reproduced with permission from Ref. [57], copyright 2022 Elsevier.

In-modified Zn (Zn@In) electrode with a scan rate of 5 mV s^{-1} [54]. The Zn@In electrode showed a higher hydrogen evolution onset potential of −1.95 V than for bare Zn (−1.84 V), suggesting the suppression of electrochemical hydrogen evolution corrosion.

Aqueous Zn corrosion produces non-conductive ZnO/Zn$(OH)_2$/ZHS and hydrogen bubbles. This should reduce the electroconductivity and increase the charge transfer resistance of Zn anodes, which can be monitored by EIS. As shown in Fig. 3c, an aged aqueous Zn anode showed greater charge transfer resistance than a fresh one [55]. Accordingly, AZMBs after 10 h of rest showed significantly lower capacity than after 10 s of rest, suggesting active Zn metal was consumed due to undesirable corrosion. This was also evaluated using the CE of Zn||Cu half cells. As indicated in Fig. 3d, a poly(vinyl butyral)-coated Zn electrode (PVB@Zn) showed an enhanced CE of 99.4%, higher than that of bare Zn (93.8%) [56].

The voltage profile of Zn||Zn symmetrical cells can also help in the analysis of Zn corrosion in AZMBs. Non-conductive corrosion products lead to polarization and increased overpotential, as shown in Fig. 3e, where a Zn electrode in liquid $ZnSO_4$ electrolyte showed a rise in voltage oscillations after 120 h of continuous cycling, while a Zn electrode modified with tannic acid (TA) and sodium alginate (SA) inhibited corrosion and exhibited stable cycling performance [57]. Note that dynamic measurement combining resting and electrochemical cycling should be more effective for evaluating the corrosion of aqueous Zn

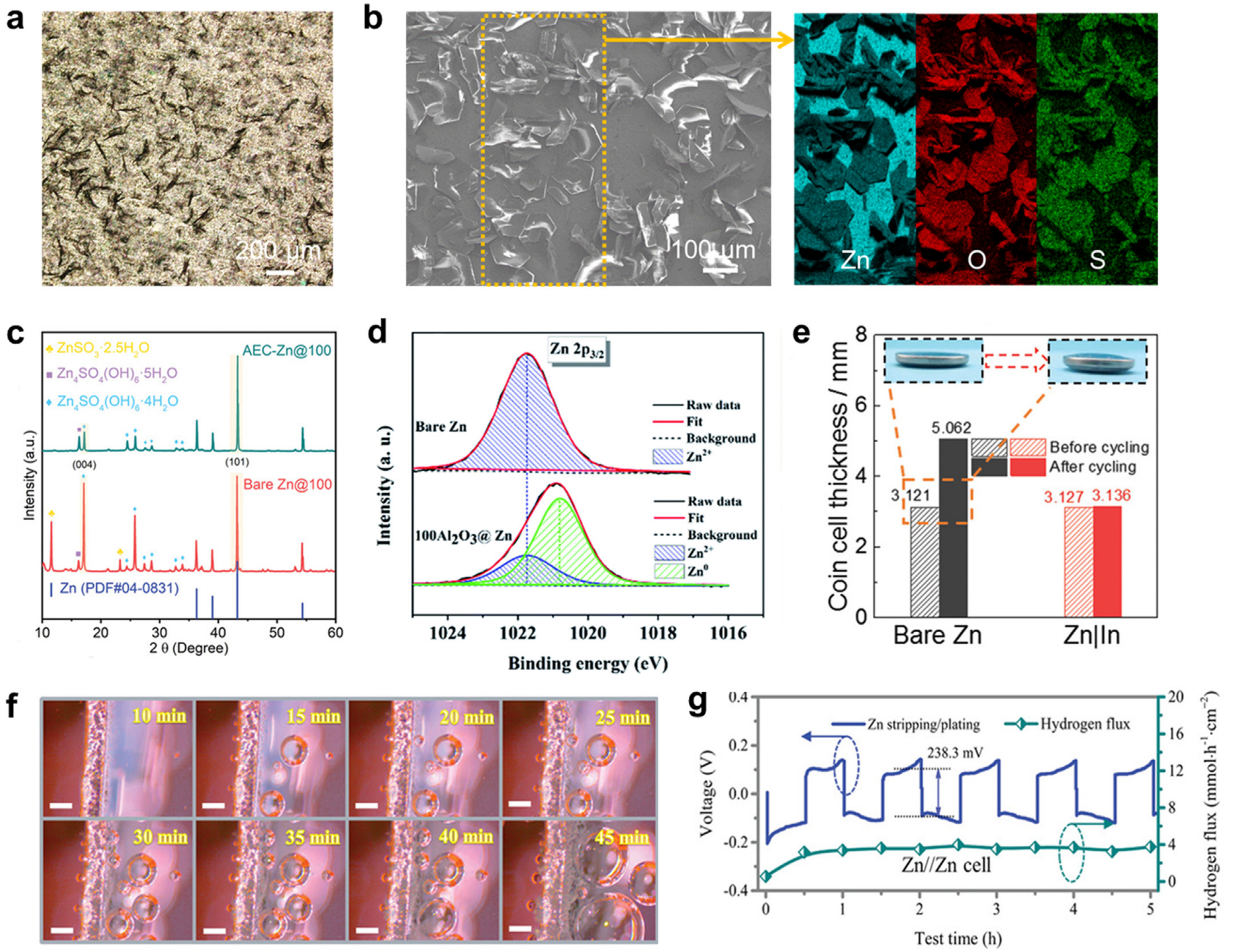

Fig. 4. (a) OM image, (b) SEM and EDS elemental mapping results for a Zn electrode after resting in $ZnSO_4$ electrolyte for 7 days. Reproduced with permission from Ref. [43], copyright 2022 Elsevier. (c) XRD patterns of Zn and anti-corrosion elastic constraint (AEC)-Zn electrodes after 100 electrochemical cycles at 0.667 mA cm^{-2} and 0.667 mAh cm^{-2}. Reproduced with permission from Ref. [58], copyright 2020 Wiley-VCH. (d) Zn 2p XPS analysis of bare Zn and $100Al_2O_3$@Zn electrodes after cycling in $Zn(SO_3CF_3)_2$ aqueous electrolyte. Reproduced with permission from Ref. [59], copyright 2020 Royal Society of Chemistry. (e) The thicknesses of Zn||Zn and Zn|In||Zn|In symmetric cells before and after cycling in $ZnSO_4$ electrolyte. Reproduced with permission from Ref. [60], copyright 2020 Wiley-VCH. (f) *In situ* OM images and (g) *in situ* monitoring of hydrogen evolution during Zn plating at 10 mA cm^{-2} in $ZnSO_4$ electrolyte. Reproduced with permission from Ref. [61], copyright 2020 Wiley-VCH.

anodes. As shown in Fig. 3f, a Zn anode in liquid $ZnSO_4$ electrolyte showed a sudden voltage fluctuation after 50 h of cycling (1.13 mA cm^{-2} and 0.28 mAh cm^{-2} for each cycle) and 60 h of resting [57], suggesting severe chemical corrosion reactions took place on the Zn electrode during resting.

3.2. Non-electrochemical methods

Zn corrosion products such as $Zn(OH)_2$ and ZHS are typical layered compounds with a sheet-like morphology, which can be observed directly under an OM. Sun et al. showed a number of sheet-like corrosion products with a size of ~200 μm by using OM to examine a Zn electrode that had rested in $ZnSO_4$ electrolyte for 7 days (Fig. 4a) [43]. SEM combined with EDS mapping can also identify these corrosion products on a Zn surface, providing clear elemental distributions (e.g., ZHS on Zn, as shown in Fig. 4b) [43]. Compared with EDS, XRD is a more powerful way to confirm the crystal structure of these corrosion products. The diffraction peaks of corrosion products like ZnO, $Zn(OH)_2$, and ZHS are generally located in the 2-theta range of 10–30° (Fig. 4c) [58]. XPS can further help to analyze the surface oxidation state of a Zn anode after corrosion reactions; a lower Zn^{2+}/Zn^0 ratio based on XPS analysis suggested a suppressed corrosion rate for a $100Al_2O_3$@Zn electrode (i.e., Zn metal coated with Al_2O_3 applied using 100 atomic layer deposition cycles) (Fig. 4d) [59].

Swelling is often observed in rested or electrochemically cycled coin cell AZMBs due to hydrogen evolution during corrosion side-reactions. The thickness of a coin cell, which can be measured with a vernier caliper, is a good indicator for evaluating the corrosion reactions in AZMBs. Kang et al. found that the thickness of a Zn||Zn symmetrical cell increased from 3.12 mm to 5.06 mm after electrochemical cycling at 0.2 mA cm^{-2} (Fig. 4e) [60]. The gas bubbles generated during electrochemical hydrogen evolution corrosion can be observed using *in situ* OM. Zhi et al. exhibited hydrogen evolution bubbles generated on bare Zn electrode in $ZnSO_4$ electrolyte at 10 mA cm^{-2} for 10 min (Fig. 4f) [61]. To accurately quantify the hydrogen evolution rate in AZMBs, Zhi et al. developed an *in situ* battery–gas chromatography–mass analysis method. The hydrogen evolution flux for a Zn||Zn symmetric cell cycling in $ZnSO_4$ electrolyte at 10 mA cm^{-2} was determined to be 4 mmol h^{-1} cm^{-2}

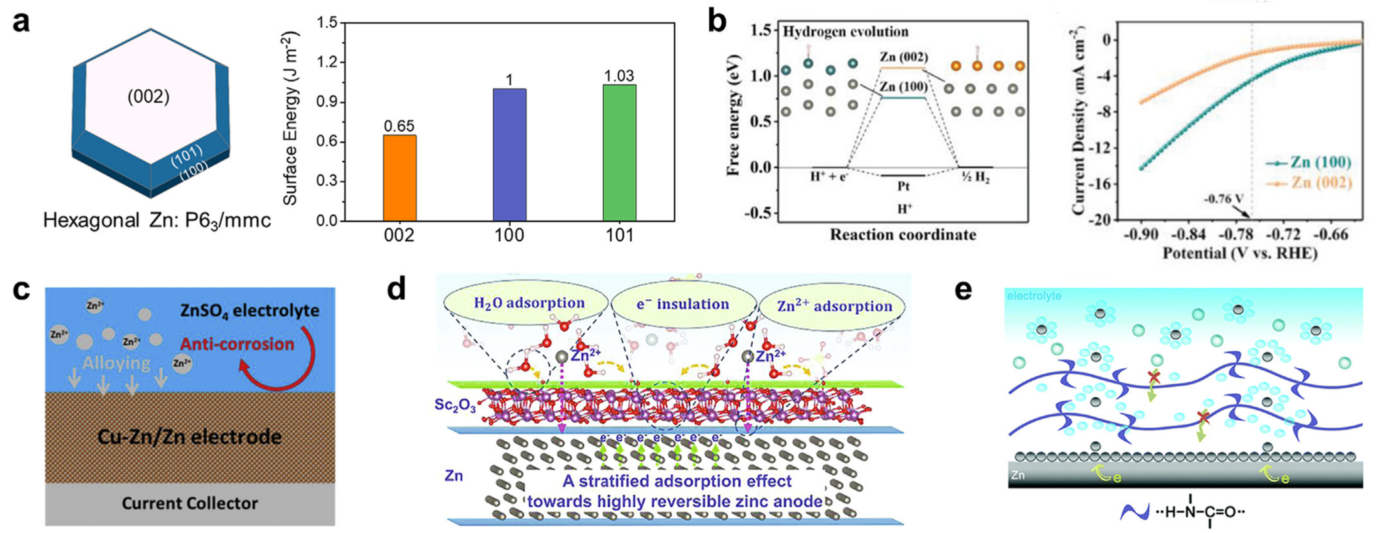

Fig. 5. (a) Surface energies for the three main planes of hexagonal Zn metal. Reproduced with permission from Ref. [43], copyright 2020 Elsevier. (b) The proton adsorption energies and linear polarization curves for electrochemical hydrogen evolution on Zn (002) and Zn (100). Reproduced with permission from Ref. [63], copyright 2021 Wiley-VCH. Schematic illustration of (c) CuZn alloy, (d) Sc_2O_3-coated Zn, and (e) PA-coated Zn electrodes with anti-corrosion capability and improved reversibility. Reproduced with permission from Ref. [36], copyright 2020 Elsevier. Reproduced with permission from Ref. [76], copyright 2021 Elsevier. Reproduced with permission from Ref. [53], copyright 2019 Royal Society of Chemistry.

(Fig. 4g) [61]. To monitor the surface corrosion/passivation and hydrogen evolution processes at the Zn/electrolyte interface, Li and co-workers developed a real-time "3 M" system based on OM, atomic force microscopy, and an electrochemical quartz crystal microbalance to capture chemical/morphological information from a corroded Zn anode in 1 M $ZnSO_4$ electrolyte. This revealed that direct contact between Zn and the electrolyte led to the formation of ZHS by-products and poor interfacial properties for aqueous Zn anodes [62].

4. Strategies for Zn corrosion protection

To prevent Zn corrosion in aqueous electrolytes and improve the reversibility of Zn anodes, plenty of strategies for Zn corrosion protection have been proposed, including texture and composition optimization, electrode structure design, and electrolyte engineering. The key to Zn corrosion protection lies in stabilizing the interface between Zn metal and aqueous electrolyte, which will be discussed in detail in this part.

4.1. Texture and composition optimization

Zn metal is a hexagonal crystal with *P*6$_3$*/mmc* symmetry. The three main crystal planes of metallic Zn are (002), (100), and (101), among which (002) is the most thermodynamically stable, with the lowest surface energy of 0.65 J m^{-2} [43]. Therefore, a Zn metal electrode with (002)-dominated facets should be the most chemically resistant (Fig. 5a). Moreover, the H adsorption free energy on Zn (002) is higher than on the other planes, endowing a (002)-Zn electrode with excellent anti-electrochemical hydrogen evolution corrosion capability, as demonstrated by the hydrogen evolution linear polarization curves of Zn(100) and Zn(002) electrodes at 1 mV s^{-1} (Fig. 5b) [63]. Therefore, regulation of the crystal planes of a metallic Zn electrode is an effective way to achieve Zn corrosion protection, and to date, several kinds of (002)-dominated Zn electrodes have been developed to achieve highly reversible Zn anodes [64–66].

With respect to composition optimization, composite electrodes with organic/inorganic functional coatings are one of the most important stabilization strategies for aqueous Zn anodes. Carbon materials such as graphene and carbon nanotubes are typical inorganic functional materials used for the surface protection of aqueous Zn anodes and the realization of corrosion-resistant performance [67,68]. A surface carbon layer isolates the active Zn and the aqueous electrolyte, thereby suppressing corrosion side-reactions. Moreover, the high electronic conductivity of carbon materials endows a carbon/Zn composite electrode with improved ion transfer kinetics and lower charge transfer resistance, which are beneficial qualities for achieving highly reversible Zn anodes.

Table 1
Summary of the anti-corrosion and electrochemical performances of aqueous Zn anodes with texture/composition optimization.

Texture/composition	I_{corr}	E_{corr}	Overpotential at 1 mA cm^{-2}
Zn(002) [63]	6186.8 μA cm^{-2}	−1.029 V	71 mV (1 mAh cm^{-2})
Cu–Zn/Zn [36]	6.03 μA cm^{-2}	−0.964 V	24 mV (0.5 mAh cm^{-2})
Zn/Cu [67]	250 μA cm^{-2}	\	20 mV (1 mAh cm^{-2})
Zn@LDH [77]	235 μA cm^{-2}	−1.015 V	38 mV (1 mAh cm^{-2})
Zn@ZnSe [78]	1690 μA cm^{-2}	\	28 mV (1 mAh cm^{-2})
MMT-Zn [79]	0.389 μA cm^{-2}	−0.743 V	50 mV (0.25 mAh cm^{-2})
Zn@ZnF$_2$ [80]	280 μA cm^{-2}	−1.014 V	36 mV (1 mAh cm^{-2})
PA-Zn [53]	312.1 μA cm^{-2}	−0.963 V	\

Alloying Zn with a chemically stable and zincophilic metal such as Cu is another strategy for protecting the surfaces of aqueous Zn anodes. The alloyed Cu not only improves the anodes' chemical stability but also promotes electrochemical Zn plating/stripping by forming a CuZn alloy (Fig. 5c) [36]. Cu foam has thus been widely accepted as a good substrate for Zn anode applications [69–71], and many CuZn alloy-based Zn electrodes have been prepared as high-performance Zn anodes [72,73]. Covering Zn anodes with a layer of a Zn^{2+}-ion conducting and electrically insulated compound (e.g., ZnS, ZnP, ZnO, Sc_2O_3, layered double hydroxide, etc.) is also beneficial for constructing anti-corrosion Zn electrodes [37,74–80]. Zhou et al. coated a homogeneous Sc_2O_3 layer on a Zn anode to suppress H_2 evolution side-reactions and achieved a high Zn plating/stripping efficiency of ~99.85% (Fig. 5d) [76]. Liang et al. constructed a carbonyl-containing layer on a Zn anode to suppress chemical oxidation corrosion, resulting in an ultralong cycling lifespan of 5000 h at 1 mA cm^{-2} and 0.25 mA cm^{-2} [81].

Besides inorganic coatings, organics with functional groups such as $-NH_2$ and $-C{=}O$ that allow Zn^{2+} transfer have also been selected for Zn surface coating and protection [55,82,83]. Cui et al. employed PA to coat a Zn metal electrode, achieving high corrosion resistance and a reversible

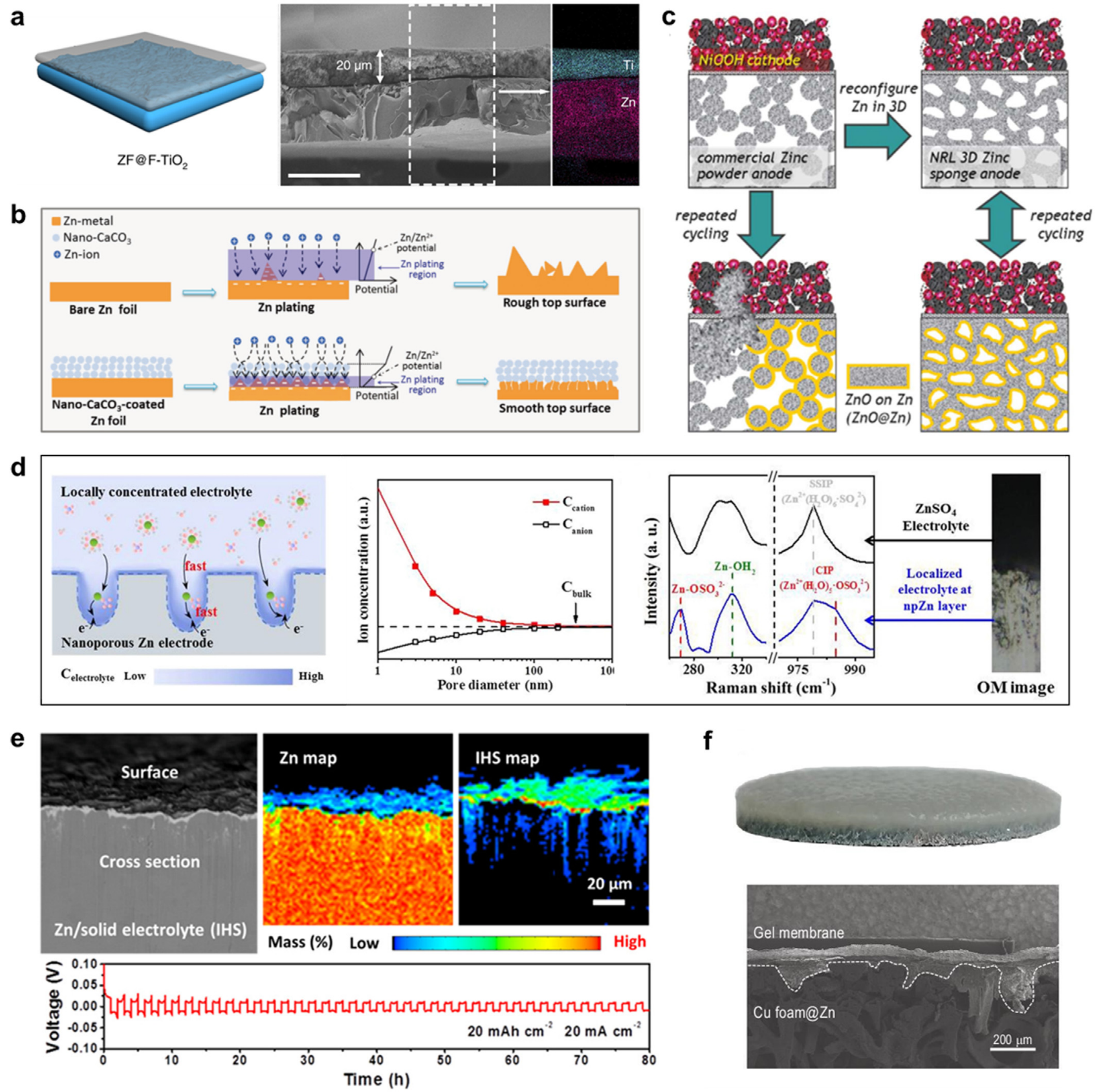

Fig. 6. (a) Schematic illustration as well as SEM and EDS elemental mapping images of a faceted TiO_2-coated Zn electrode. Reproduced with permission from Ref. [87], copyright 2020 Springer Nature. (b) Schematic illustration of highly-reversible nano $CaCO_3$-coated Zn electrode in $ZnSO_4$ electrolyte. Reproduced with permission from Ref. [88], copyright 2018 Wiley-VCH. (c) Schematic illustration of 3D Zn sponge electrode in KOH electrolyte. Reproduced with permission from Ref. [23], copyright 2017 American Association for the Advancement of Science. (d) Schematic illustration, theoretical simulation, and Raman spectra results for localized concentrated electrolyte on 3D porous Zn electrode in $ZnSO_4$ electrolyte. Reproduced with permission from Ref. [90], copyright 2021 Elsevier. (e) High-precision electron probe microanalysis and voltage profile of 3D interdigitated Zn/IHS electrode. Reproduced with permission from Ref. [91], copyright 2021 American Chemical Society. (f) Schematic and SEM image of 3D gel/Cu foam@Zn electrode. Reproduced with permission from Ref. [71], copyright 2022 Oxford Academic.

PA-coated Zn anode in aqueous batteries (Fig. 5e) [53]. Zhang et al. introduced a layer of sericin molecules on a Zn anode, which exhibited greater overpotential due to reduced electrochemical hydrogen evolution corrosion and had a prolonged cycling lifetime of 4446 h at 1 mA cm^{-2} and 1 mAh cm^{-2} [84].

To compare the effectiveness of the above texture and composition optimization strategies, the anti-corrosion and electrochemical performances of as-optimized Zn electrodes are summarized in Table 1. Notably, while organic/inorganic coating layers have shown many advantages in suppressing Zn corrosion reactions, the thicknesses of these surface layers are generally very large (> 1 μm); this is not conducive to Zn^{2+}-ion transfer during the Zn plating/stripping processes and prevents further performance optimization of aqueous Zn anodes.

Table 2
Summary of the anti-corrosion and electrochemical performances of aqueous Zn anodes with various electrode structures.

Electrode structure	I_{corr}	E_{corr}	Overpotential at 1 mA cm^{-2}
2D ZnF_2/Ag@Zn [92]	\	−1.042 V	25 mV (1 mAh cm^{-2})
2D DES-Zn [93]	3500 μA cm^{-2}	−1.021 V	30 mV (0.5 mAh cm^{-2})
2D Zn/ex-ZrP [94]	210 μA cm^{-2}	−1.02 V	\
3D Zn@a-Ag [95]	1.08 μA cm^{-2}	−1.018 V	\
3D npZn [90]	4000 μA cm^{-2}	−0.975 V	25 mV (1 mAh cm^{-2})
3D Zn/IHS [91]	\	\	10 mV (0.5 mAh cm^{-2})
2D ZSM-5@Zn [96]	1300 μA cm^{-2}	−0.978 V	45 mV (1 mAh cm^{-2})

4.2. Electrode structure design

As noted above, a surface protective layer is often employed to suppress Zn corrosion and achieve highly reversible aqueous Zn anodes. The surface protective layer is two-dimensional (2D) in most cases. Polymer electrolytes can serve as a 2D protective layer to stabilize aqueous Zn anodes against corrosion reactions. Kim et al. coated a thin polysiloxane layer ($<$ 500 nm) on Zn as an artificial solid–electrolyte interface to inhibit corrosion reactions and achieve a remarkable cycling stability of 600 h at 20 mA cm^{-2} and 5 mAh cm^{-2} [85]. Compared to a polymer coating, a native passivation layer on a Zn anode reported by Huang et al. showed advantages, including strong adhesion to Zn and high homogeneity, thus enabling a cycle life up to 40 times longer than a bare Zn electrode at 1 mA cm^{-2} and 1 mA h cm^{-2} [86].

Importantly, the facets of coating materials play a vital role in determining the efficiency of a surface protective layer. Wang et al. introduced an oriented TiO_2 protective layer with a (001) facet on a Zn electrode [87], which exhibited good cycling stability for more than 450 h at 1 mA cm^{-2} and 1 mAh cm^{-2} (Fig. 6a). Zn^{2+}-ion flux should also be paid particular attention when designing 2D protective layers. Liang et al. applied a nano-$CaCO_3$ coating layer to reduce the contact between metallic Zn and aqueous electrolyte, as well as regulate the Zn^{2+}-ion flux [88], thus enabling a highly reversible Zn metal electrode in $ZnSO_4$ + $MnSO_4$ aqueous electrolyte (Fig. 6b).

Notably, the electrochemical surface area of a Zn metal electrode cannot be improved by designing the 2D electrode structure, which is detrimental for achieving high-power AZMB anodes. Hence, designing and fabricating a three-dimensional (3D) Zn electrode is quite necessary [89]. Rolison et al. prepared a 3D zinc sponge anode and achieved high-power alkaline nickel–zinc cells for more than 100 high-rate cycles (Fig. 6c) [23]. However, a 3D Zn electrode with an enlarged surface area experiences an increased corrosion rate. This situation is not so serious in alkaline nickel–zinc cells, since amphoteric ZnO is soluble in alkaline electrolytes. But with a neutral electrolyte, a 3D porous Zn electrode with an enlarged surface area should show poor electrochemical reversibility due to aggravated corrosion side-reactions. To address this issue, Sun et al. regulated the space charge distribution within a 3D Zn electrode with an accurately controlled nanopore structure [90]. They revealed that the cation concentration at the electric double-layer was significantly higher than in the bulk electrolyte for a porous Zn electrode with a nanopore size smaller than 40 nm. Raman studies confirmed there was a lower H_2O/Zn^{2+} ratio and a higher concentration of Zn^{2+} cations in the nanoporous layer than in the bulk $ZnSO_4$ electrolyte (Fig. 6d), resulting in suppressed corrosion and enhanced reversibility of the 3D nanoporous Zn anode.

Another way to construct a 3D Zn electrode is to employ a replacement reaction to fabricate an interdigitated metal/solid electrolyte electrode. For example, In metal was deposited along the grain boundary of polycrystalline Zn via a simple replacement reaction. After electrochemical activation, the as-deposited In metal was transformed into indium hydroxide sulfate (IHS) solid electrolyte, enabling a 3D interdigitated Zn/IHS electrode [91]. The interdigitated IHS solid electrolyte not only isolated active Zn with liquid electrolyte, suppressing corrosion side-reactions, but also endowed the Zn electrode with an enlarged surface area, thus achieving remarkable reversibility in $ZnSO_4$ electrolyte at 20 mA cm^{-2} and 20 mAh cm^{-2} (Fig. 6e). In addition, Liang and co-workers proposed an integrated “all-in-one” strategy to design a 3D electrode structure by combining a Cu foam@Zn electrode and gel quasi-solid electrolyte [71]. This showed anti-corrosion properties and achieved 60 h of shelving stability and 1200 electrochemical cycles at 1 mA cm^{-2} and 0.48 mAh cm^{-2} (Fig. 6f). Table 2 compares the anti-corrosion and electrochemical performances of Zn electrodes protected using various electrode structural design strategies. Note that the fabrication of 3D electrodes generally involves complicated processes that are hard to control and scale up, which is very detrimental to the practical application of these 3D Zn anodes.

4.3. Electrolyte engineering

Electrolyte engineering is a facile and scalable method for suppressing the corrosion of aqueous Zn anodes by decreasing the content/activity of free water in the electrolyte. It has been found that water molecules are spontaneously absorbed on the surface of metallic Zn [97], triggering corrosion reactions between active Zn and aqueous electrolytes. An electrolyte additive is one of the most typical electrolyte engineering strategies for preventing Zn corrosion [98–104]. For example, ethylene diamine tetraacetic acid (EDTA) additive in aqueous $ZnSO_4$ electrolyte is absorbed on Zn instead of water (Fig. 7a), thus reducing the corrosion rate and enabling stable electrochemical performance for 5000 h under dynamic measurement combining electrochemical cycling (1 mA cm^{-2}, 0.5 mAh cm^{-2}, 72 h) with resting (24 h) [97].

The corrosion rate of an aqueous Zn electrode can also be reduced by decreasing the free water content in the aqueous electrolyte [44, 105–107]. Tao et al. employed a water/dimethyl sulfoxide hybrid solvent to prepare aqueous electrolyte with reduced free water content, which increased the hydrogen evolution overpotential and enabled highly reversible aqueous batteries (Fig. 7b) [108]. Wang et al. put forward a “water-in-salt” electrolyte strategy (i.e., 1 M $Zn(TFSI)_2$ + 20 M LiTFSI). The Zn^{2+}-solvation structure was finely regulated (5–20 M, Fig. 7c), thus producing a highly reversible Zn anode with a stable CE of $>$ 99.7% [21].

In another approach, deep eutectic solvents, which have high solubility for Zn salt and are generally in a liquid state at room temperature, can be used as AZMB electrolytes to inhibit the corrosion of Zn anodes [109]. Chen et al. reported a “water-in-deep eutectic solvent” electrolyte, namely a eutectic mixture of urea, $Zn(N(SO_2CF_3)_2)_2$, and $LiN(SO_2CF_3)_2$ with 30 mol% H_2O, wherein all the H_2O molecules were H-bonded and coordinated in the internal network of the deep eutectic solvent, resulting in suppressed corrosion reactions and reversible Zn plating/stripping performance [110]. Cui et al. developed a non-aqueous eutectic acetamide-$Zn(TFSI)_2$ electrolyte to construct a stable organic/inorganic hybrid interphase for a reversible Zn electrode with ~100% CE (Fig. 7d) [111].

Table 3 compares the anti-corrosion and electrochemical performances of Zn electrodes in various electrolytes in recent publications. The main limitation upon using these electrolyte engineering strategies in next-generation AZMBs for grid-scale energy storage is that they commonly employ costly salts/additives or toxic organic solvents.

5. Conclusion and outlook

In summary, we have reviewed the corrosion mechanisms of aqueous Zn anodes in both alkaline and neutral batteries, the methods for studying aqueous Zn corrosion, and the surface protection strategies for generating anti-corrosion Zn anodes. Since the performance of practical AZMBs has thus far been limited by issues at the Zn anode, we call for intense research activities on aqueous Zn chemistry, especially the corrosion issue, to achieve the further development of advanced AZMBs. The potential future research challenges and directions we believe to be important for making corrosion-resistant AZMBs a commercial reality are summarized as follows.

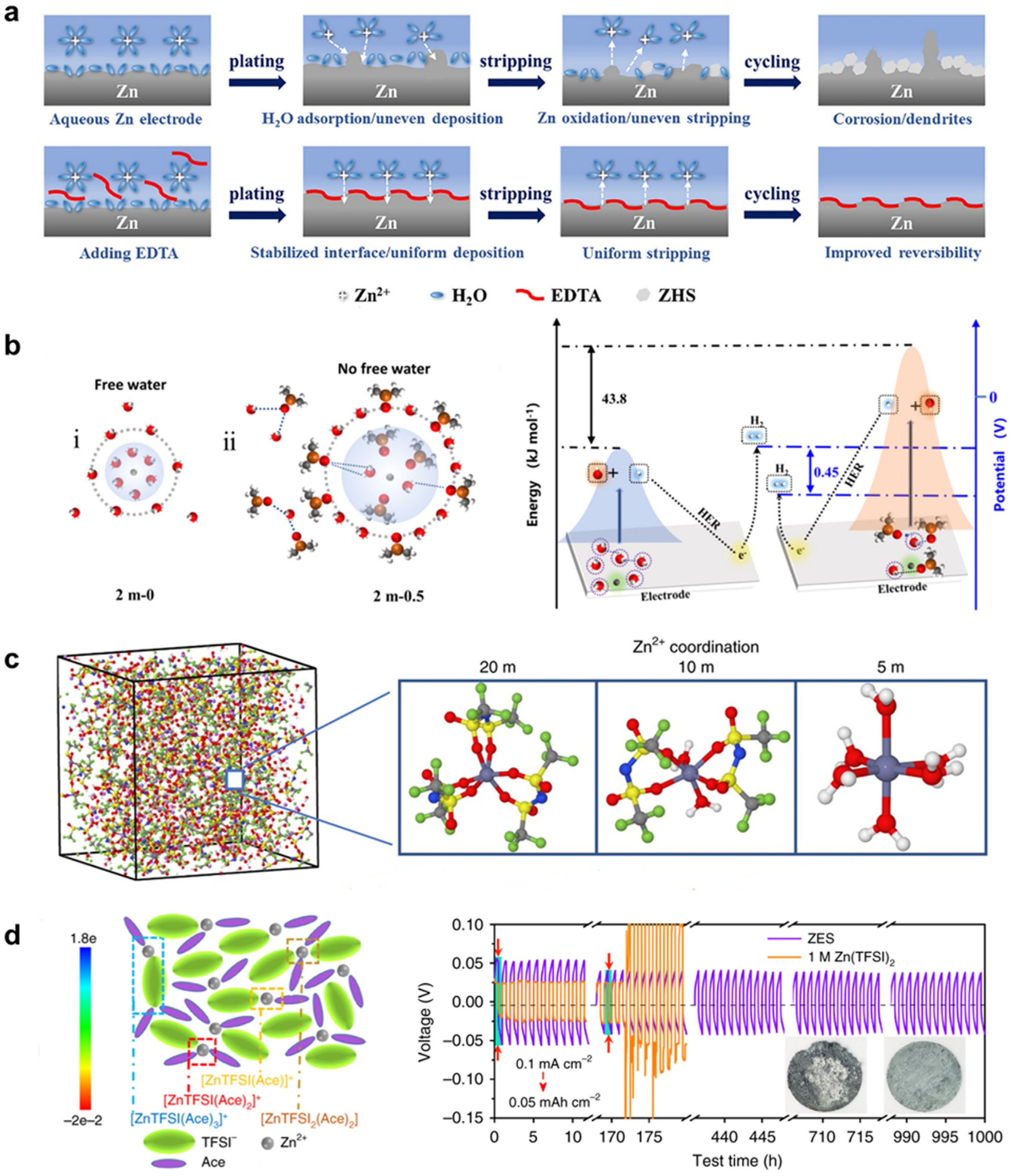

Fig. 7. Schematic illustration of the functionality of (a) EDTA electrolyte additive, (b) water/dimethyl sulfoxide hybrid solvent, (c) high-concentration electrolyte (1 M $Zn(TFSI)_2$ + 20 M LiTFSI), and (d) $Zn(TFSI)_2$-based eutectic solvent for anti-corrosion aqueous Zn anodes. Reproduced with permission from Ref. [97], copyright 2021 Wiley-VCH. Reproduced with permission from Ref. [108], copyright 2021 American Chemical Society. Reproduced with permission from Ref. [21], copyright 2018 Springer Nature. Reproduced with permission from Ref. [111], copyright 2022 Springer Nature.

Table 3
Summary of the anti-corrosion and electrochemical performances of aqueous Zn anodes with electrolyte engineering.

Electrolyte	I_{corr}	E_{corr}	Overpotential at 1 mA cm^{-2}	Refs.
Zn $(CF_3SO_3)_2$ + $Zn(H_2PO_4)_2$	372.6 μA cm^{-2}	−9.045 V	40 mV (1 mAh cm^{-2})	[100]
$ZnSO_4$ + glucose	590 μA cm^{-2}	\	70 mV (1 mAh cm^{-2})	[104]
$ZnSO_4$ + EDTA	1180 μA cm^{-2}	−0.989 V	25 mV (0.5 mAh cm^{-2})	[97]
$ZnSO_4$ + $La(NO_3)_3$	6.3 μA cm^{-2}	−0.958 V	45 mV (1 mAh cm^{-2})	[112]
$Zn(OTf)_2$ in DMF/H_2O	410 μA cm^{-2}	−0.975 V	\	[113]
PG + $ZnSO_4$	190 μA cm^{-2}	−1.005 V	100 mV (1 mAh cm^{-2})	[114]
DPA + $ZnSO_4$	22 μA cm^{-2}	\	35 mV (1 mAh cm^{-2})	[115]

(1) *In situ* characterization techniques should be developed and utilized to gain a deep understanding of Zn corrosion, especially at the molecular or atomic level, and thereby provide a theoretical basis for Zn corrosion protection.
(2) Researchers need to optimize the alignment between their methods and improve the overall performance of AZMBs, rather than merely focus on corrosion-resistance performance.
(3) Anode corrosion behavior and battery performance should be evaluated under limiting conditions such as high (60–90 °C) and sub-zero temperatures, in light of practical application scenarios for AZMBs such as in deserts or extremely cold places.
(4) The development of modification methods to achieve anti-corrosion Zn anodes that are green, low-cost, and scalable should greatly benefit the practical application of next-generation AZMBs with high energy density and long cycle life.

Declaration of competing interest

The authors declare no competing financial interests.

Acknowledgments

Y. Sun acknowledges the financial support by the Innovation Fund of Wuhan National Laboratory for Optoelectronics of Huazhong University of Science and Technology. Z. Cai acknowledges the financial support from the National Natural Science Foundation of China (No. 22205068). The project was supported by the "CUG Scholar" Scientific Research Funds at China University of Geosciences (Wuhan) (Project No.2022118).

References

[1] Y. Guo, S. Wu, Y.-B. He, F. Kang, L. Chen, H. Li, Q.-H. Yang, Solid-state lithium batteries: safety and prospects, eScience 2 (2022) 138–163.
[2] L. Fu, X. Wang, L. Wang, M. Wan, Y. Li, Z. Cai, Y. Tan, G. Li, R. Zhan, Z.W. Seh, Y. Sun, A salt-in-metal anode: stabilizing the solid electrolyte interphase to enable prolonged battery cycling, Adv. Funct. Mater. 31 (2021) 2010602.
[3] X. Liu, T. Liu, R. Wang, Z. Cai, W. Wang, Y. Yuan, R. Shahbazian-Yassar, X. Li, S. Wang, E. Hu, X.-Q. Yang, Y. Xiao, K. Amine, J. Lu, Y. Sun, Prelithiated Li-enriched gradient interphase toward practical high-energy NMC-silicon full cell, ACS Energy Lett. 6 (2021) 320–328.
[4] J. Huang, J. Zhou, S. Liang, Guest pre-intercalation strategy to boost the electrochemical performance of aqueous zinc-ion battery cathodes, Acta Phys. Chim. Sin. 37 (2021) 2005020.
[5] S. Zhang, L. Sun, Q. Fan, F. Zhang, Z. Wang, J. Zou, S. Zhao, J. Mao, Z. Guo, Challenges and prospects of lithium-CO_2 batteries, Nano Res. Energy 1 (2022) e9120001.
[6] Z. Wang, M. Zhou, L. Qin, M. Chen, Z. Chen, S. Guo, L. Wang, G. Fang, S. Liang, Simultaneous regulation of cations and anions in an electrolyte for high-capacity, high-stability aqueous zinc-vanadium batteries, eScience 2 (2022) 209–218.
[7] Z. Liu, X. Luo, L. Qin, G. Fang, S. Liang, Progress and prospect of low-temperature zinc metal batteries, Adv. Powder Mater. 1 (2022) 100011.
[8] A. Konarov, N. Voronina, J.H. Jo, Z. Bakenov, Y.K. Sun, S.T. Myung, Present and future perspective on electrode materials for rechargeable zinc-ion batteries, ACS Energy Lett. 3 (2018) 2620–2640.
[9] Z. Cai, J. Wang, Z. Lu, R. Zhan, Y. Ou, L. Wang, M. Dahbi, J. Alami, J. Lu, K. Amine, Y. Sun, Ultrafast metal electrodeposition revealed by in situ optical imaging and theoretical modeling towards fast-charging Zn battery chemistry, Angew. Chem. Int. Ed. 61 (2022) e202116560.
[10] G. Fang, J. Zhou, A. Pan, S. Liang, Recent advances in aqueous zinc-ion batteries, ACS Energy Lett. 3 (2018) 2480–2501.
[11] J. Hao, X. Li, X. Zeng, D. Li, J. Mao, Z. Guo, Deeply understanding the Zn anode behavior and corresponding improvement strategies in different aqueous Zn-based batteries, Energy Environ. Sci. 13 (2020) 3917–3949.
[12] Y. Li, B. Liu, J. Ding, X. Han, Y. Deng, T. Wu, K. Amine, W. Hu, C. Zhong, J. Lu, Understanding the gap between academic research and industrial requirements in rechargeable zinc-ion batteries, Batteries Supercaps 4 (2020) 60–71.
[13] B. Scrosati, History of lithium batteries, J. Solid State Electrochem. 15 (2011) 1623–1630.
[14] J. Phillips, S. Mohanta, M. Geng, J. Barton, B. McKinney, J. Wu, Environmentally friendly nickel-zinc battery for high rate applications with higher specific energy, ECS Trans. 16 (2009) 11–17.
[15] X. Chen, Z. Zhou, H.E. Karahan, Q. Shao, L. Wei, Y. Chen, Recent advances in materials and design of electrochemically rechargeable zinc-air batteries, Small 14 (2018) 1801929.
[16] V. Yufit, F. Tariq, D.S. Eastwood, M. Biton, B. Wu, P.D. Lee, N.P. Brandon, Operando visualization and multi-scale tomography studies of dendrite formation and dissolution in zinc batteries, Joule 3 (2019) 485–502.
[17] T. Yamamoto, T. Shoji, Rechargeable ZnlZnSO$_4$lMnO$_2$-type cells, Inorg. Chim. Acta. 117 (1986) L27–L28.
[18] X. Shen, X. Wang, N. Yu, W. Yang, Y. Zhou, Y. Shi, Y. Wang, L. Dong, J. Di, Q. Li, A polypyrrole-coated MnO_2 carbon nanotube film cathode for rechargeable aqueous Zn-ion batteries, Acta Phys. Chim. Sin. 38 (2022) 2006059.
[19] Y. Heng, Z. Gu, J. Guo, X. Wu, Research progresses on vanadium-based cathode materials for aqueous zinc-ion batteries, Acta Phys. Chim. Sin. 37 (2021) 2005013.
[20] L. Zhang, L. Chen, X. Zhou, Z. Liu, Towards high-voltage aqueous metal-ion batteries beyond 1.5 V: the zinc/zinc hexacyanoferrate system, Adv. Energy Mater. 5 (2015) 1400930.
[21] F. Wang, O. Borodin, T. Gao, X. Fan, W. Sun, F. Han, A. Faraone, J.A. Dura, K. Xu, C. Wang, Highly reversible zinc metal anode for aqueous batteries, Nat. Mater. 17 (2018) 543–549.
[22] D. Han, C. Cui, K. Zhang, Z. Wang, J. Gao, Y. Guo, Z. Zhang, S. Wu, L. Yin, Z. Weng, F. Kang, Q.H. Yang, A non-flammable hydrous organic electrolyte for sustainable zinc batteries, Nat. Sustain. 5 (2022) 205–213.
[23] J.F. Parker, C.N. Chervin, I.R. Pala, M. Machler, M.F. Burz, J.W. Long, D.R. Rolison, Rechargeable nickel-3D zinc batteries: an energy-dense, safer alternative to lithium-ion, Science 356 (2017) 415–418.
[24] Y. Li, H. Dai, Recent advances in zinc-air batteries, Chem. Soc. Rev. 43 (2014) 5257–5275.
[25] C. Xu, B. Li, H. Du, F. Kang, Energetic zinc ion chemistry: the rechargeable zinc ion battery, Angew. Chem. Int. Ed. 51 (2012) 933–935.
[26] D. Kundu, B.D. Adams, V. Duffort, S.H. Vajargah, L.F. Nazar, A high-capacity and long-life aqueous rechargeable zinc battery using a metal oxide intercalation cathode, Nat. Energy 1 (2016) 16119.
[27] L.E. Blanc, D. Kundu, L.F. Nazar, Scientific challenges for the implementation of Zn-ion batteries, Joule 4 (2020) 771–799.
[28] T.C. Li, D. Fang, J. Zhang, M.E. Pam, Z.Y. Leong, J. Yu, X.L. Li, D. Yan, H.Y. Yang, Recent progress in aqueous zinc-ion batteries: a deep insight into zinc metal anodes, J. Mater. Chem. 9 (2021) 6013–6028.
[29] J. Shin, J. Lee, Y. Park, J.W. Choi, Aqueous zinc ion batteries: focus on zinc metal anodes, Chem. Sci. 11 (2020) 2028–2044.
[30] H. Wang, R. Tan, Z. Yang, Y. Feng, X. Duan, J. Ma, Stabilization perspective on metal anodes for aqueous batteries, Adv. Energy Mater. 11 (2020) 2000962.
[31] M. Wang, Y. Meng, K. Li, T. Ahmad, N. Chen, Y. Xu, J. Sun, M. Chuai, X. Zheng, Y. Yuan, C. Shen, Z. Zhang, W. Chen, Toward dendrite-free and anti-corrosion Zn anodes by regulating a bismuth-based energizer, eScience 2 (2022) 509–517.
[32] W. Du, E.H. Ang, Y. Yang, Y. Zhang, M. Ye, C. Li, Challenges in material and structure design of zinc anode toward high-performance aqueous zinc-ion batteries, Energy Environ. Sci. 13 (2020) 3330–3360.
[33] D. Chao, W. Zhou, F. Xie, C. Ye, H. Li, M. Jaroniec, S.Z. Qiao, Roadmap for advanced aqueous batteries: from design of materials to applications, Sci. Adv. 6 (2020) eaba4098.
[34] J. Fu, R.L. Liang, G.H. Liu, A.P. Yu, Z.Y. Bai, L. Yang, Z.W. Chen, Recent progress in electrically rechargeable zinc-air batteries, Adv. Mater. 31 (2018) e1805230.
[35] J. Huang, Z. Guo, Y. Ma, D. Bin, Y. Wang, Y. Xia, Recent progress of rechargeable batteries using mild aqueous electrolytes, Small Methods 3 (2019) 1800272.
[36] Z. Cai, Y. Ou, J. Wang, R. Xiao, L. Fu, Z. Yuan, R. Zhan, Y. Sun, Chemically resistant Cu-Zn/Zn composite anode for long cycling aqueous batteries, Energy Stor. Mater. 27 (2020) 205–211.

[37] J. Hao, B. Li, X. Li, X. Zeng, S. Zhang, F. Yang, S. Liu, D. Li, C. Wu, Z. Guo, An in-depth study of Zn metal surface chemistry for advanced aqueous Zn-ion batteries, Adv. Mater. 32 (2020) 2003021.

[38] D. Li, L. Cao, T. Deng, S. Liu, C. Wang, Design of a solid electrolyte interphase for aqueous Zn batteries, Angew. Chem. Int. Ed. 60 (2021) 13035–13041.

[39] P. Liang, J. Yi, X. Liu, K. Wu, Z. Wang, J. Cui, Y. Liu, Y. Wang, Y. Xia, J. Zhang, Highly reversible Zn anode enabled by controllable formation of nucleation sites for Zn-based batteries, Adv. Funct. Mater. 30 (2020) 1908528.

[40] Y. Shi, Y. Chen, L. Shi, K. Wang, B. Wang, L. Li, Y. Ma, Y. Li, Z. Sun, W. Ali, S. Ding, An overview and future perspectives of rechargeable zinc batteries, Small 16 (2020) 2000730.

[41] Y. Zhang, Y. Wu, W. You, M. Tian, P.W. Huang, Y. Zhang, Z. Sun, Y. Ma, T. Hao, N. Liu, Deeply rechargeable and hydrogen-evolution-suppressing zinc anode in alkaline aqueous electrolyte, Nano Lett. 20 (2020) 4700–4707.

[42] V. Verma, S. Kumar, W. Manalastas, M. Srinivasan, Undesired reactions in aqueous rechargeable zinc ion batteries, ACS Energy Lett. 6 (2021) 1773–1785.

[43] J. Wang, B. Zhang, Z. Cai, R. Zhan, W. Wang, L. Fu, M. Wan, R. Xiao, Y. Ou, L. Wang, J. Jiang, Z.W. Seh, H. Li, Y. Sun, Stable interphase chemistry of textured Zn anode for rechargeable aqueous batteries, Sci. Bull. 67 (2022) 716–724.

[44] C. Liu, X. Xie, B. Lu, J. Zhou, S. Liang, Electrolyte strategies toward better zinc-ion batteries, ACS Energy Lett. 6 (2021) 1015–1033.

[45] W. Lu, C. Zhang, H. Zhang, X. Li, Anode for zinc-based batteries: challenges, strategies, and prospects, ACS Energy Lett. 6 (2021) 2765–2785.

[46] M. Pourbaix, Atlas of Electrochemical Equilibria in Aqueous Solutions, National Association of Corrosion Engineers, 1974, p. 307.

[47] Q. Li, Y. Wang, F. Mo, D. Wang, G. Liang, Y. Zhao, Q. Yang, Z. Huang, C. Zhi, Calendar life of Zn batteries based on Zn anode with Zn powder/current collector structure, Adv. Energy Mater. 11 (2021) 2003931.

[48] A. Bayaguud, Y. Fu, C. Zhu, Interfacial parasitic reactions of zinc anodes in zinc ion batteries: underestimated corrosion and hydrogen evolution reactions and their suppression strategies, J. Energy Chem. 64 (2022) 246–262.

[49] L. Zhang, Y. Hou, Comprehensive analyses of aqueous Zn metal batteries: characterization methods, simulations, and theoretical calculations, Adv. Energy Mater. 11 (2021) 2003823.

[50] L. Kang, M. Cui, Z. Zhang, F. Jiang, Rechargeable aqueous zinc ion batteries with mild electrolytes: a comprehensive review, Batteries & Supercaps. 3 (2020) 966–1005.

[51] A. Bayaguud, X. Luo, Y. Fu, C. Zhu, Cationic surfactant-type electrolyte additive enables three-dimensional dendrite-free zinc anode for stable zinc-ion batteries, ACS Energy Lett. 5 (2020) 3012–3020.

[52] C. Deng, X. Xie, J. Han, Y. Tang, J. Gao, C. Liu, X. Shi, J. Zhou, S. Liang, A sieve-functional and uniform-porous kaolin layer toward stable zinc metal anode, Adv. Funct. Mater. 30 (2020) 2000599.

[53] Z. Zhao, J. Zhao, Z. Hu, J. Li, J. Li, Y. Zhang, C. Wang, G. Cui, Long-life and deeply rechargeable aqueous Zn anodes enabled by a multifunctional brightener-inspired interphase, Energy Environ. Sci. 12 (2019) 1938–1949.

[54] P. Xiao, H. Li, J. Fu, C. Zeng, Y. Zhao, T. Zhai, H. Li, An anticorrosive zinc metal anode with ultra-long cycle life over one year, Energy Environ. Sci. 15 (2022) 1638–1646.

[55] M. Zhu, J. Hu, Q. Lu, H. Dong, D.D. Karnaushenko, C. Becker, D. Karnaushenko, Y. Li, H. Tang, Z. Qu, J. Ge, O.G. Schmidt, A patternable and in situ formed polymeric zinc blanket for a reversible zinc anode in a skin-mountable microbattery, Adv. Mater. 33 (2021) 2007497.

[56] J. Hao, X. Li, S. Zhang, F. Yang, X. Zeng, S. Zhang, G. Bo, C. Wang, Z. Guo, Designing dendrite-free zinc anodes for advanced aqueous zinc batteries, Adv. Funct. Mater. 30 (2020) 2001263.

[57] B. Zhang, L. Qin, Y. Fang, Y. Chai, X. Xie, B. Lu, S. Liang, J. Zhou, Tuning Zn^{2+} coordination tunnel by hierarchical gel electrolyte for dendrite-free zinc anode, Sci. Bull. 67 (2022) 955–962.

[58] R. Zhao, Y. Yang, G. Liu, R. Zhu, J. Huang, Z. Chen, Z. Gao, X. Chen, L. Qie, Redirected Zn electrodeposition by an anti-corrosion elastic constraint for highly reversible Zn anodes, Adv. Funct. Mater. 31 (2020) 2001867.

[59] H. He, H. Tong, X. Song, X. Song, J. Liu, Highly stable Zn metal anodes enabled by atomic layer deposited Al_2O_3 coating for aqueous zinc-ion batteries, J. Mater. Chem. A 8 (2020) 7836–7846.

[60] D. Han, S. Wu, S. Zhang, Y. Deng, C. Cui, L. Zhang, Y. Long, H. Li, Y. Tao, Z. Weng, Q.H. Yang, F. Kang, A corrosion-resistant and dendrite-free zinc metal anode in aqueous systems, Small 16 (2020) 2001736.

[61] L. Ma, Q. Li, Y. Ying, F. Ma, S. Chen, Y. Li, H. Huang, C. Zhi, Toward practical high-areal-capacity aqueous zinc-metal batteries: quantifying hydrogen evolution and a solid-ion conductor for stable zinc anodes, Adv. Mater. 33 (2021) 2007406.

[62] X. Zhou, Y. Lu, Q. Zhang, L. Miao, K. Zhang, Z. Yan, F. Li, J. Chen, Exploring the interfacial chemistry between zinc anodes and aqueous electrolytes via an in situ visualized characterization system, ACS Appl. Mater. Interfaces 12 (2020) 55476–55482.

[63] M. Zhou, S. Guo, J. Li, X. Luo, Z. Liu, T. Zhang, X. Cao, M. Long, B. Lu, A. Pan, G. Fang, J. Zhou, S. Liang, Surface-preferred crystal plane for a stable and reversible zinc anode, Adv. Mater. 33 (2021) 2100187.

[64] J.X. Zheng, Y. Deng, J.F. Yin, T. Tang, R. Garcia-Mendez, Q. Zhao, L.A. Archer, Textured electrodes: manipulating built-in crystallographic heterogeneity of metal electrodes via severe plastic deformation, Adv. Mater. 34 (2021) 2106867.

[65] S.D. Pu, C. Gong, Y.T. Tang, Z. Ning, J. Liu, S. Zhang, Y. Yuan, D. Melvin, S. Yang, L. Pi, J.J. Marie, B. Hu, M. Jenkins, Z. Li, B. Liu, S.C.E. Tsang, T.J. Marrow, R.C. Reed, X. Gao, P.G. Bruce, A.W. Robertson, Achieving ultrahigh-rate planar and dendrite-free zinc electroplating for aqueous zinc battery anodes, Adv. Mater. 34 (2022) 2202552.

[66] D. Yuan, J. Zhao, H. Ren, Y. Chen, R. Chua, E.T.J. Jie, Y. Cai, E. Edison, W. Manalastas Jr., M.W. Wong, M. Srinivasan, Anion texturing towards dendrite-free Zn anode for aqueous rechargeable batteries, Angew. Chem. Int. Ed. 60 (2021) 7213–7219.

[67] H. Wang, Y. Chen, H. Yu, W. Liu, G. Kuang, L. Mei, Z. Wu, W. Wei, X. Ji, B. Qu, L. Chen, A multifunctional artificial interphase with fluorine-doped amorphous carbon layer for ultra-stable Zn anode, Adv. Funct. Mater. 32 (2022) 2205600.

[68] Y. Su, X. Yang, Q. Zhang, J. Sun, Z. Liu, Carbon nanomaterials for highly stable Zn anode: recent progress and future outlook, J. Electroanal. Chem. 904 (2022) 115883.

[69] Q. Zhang, J. Luan, L. Fu, S. Wu, Y. Tang, X. Ji, H. Wang, The three-dimensional dendrite-free zinc anode on a copper mesh with a zinc-oriented polyacrylamide electrolyte additive, Angew. Chem. Int. Ed. 58 (2019) 15841–15847.

[70] X. Shi, G. Xu, S. Liang, C. Li, S. Guo, X. Xie, X. Ma, J. Zhou, Homogeneous deposition of zinc on three-dimensional porous copper foam as a superior zinc metal anode, ACS Sustainable Chem. Eng. 7 (2019) 17737–17746.

[71] C. Li, X. Xie, H. Liu, P. Wang, C. Deng, B. Lu, J. Zhou, S. Liang, Integrated ‘all-in-one’ strategy to stabilize zinc anodes for high-performance zinc-ion batteries, Natl. Sci. Rev. 9 (2022) nwab177.

[72] M. Fayette, H.J. Chang, I.A. Rodri Guez-Perez, X. Li, D. Reed, Electrodeposited zinc-based films as anodes for aqueous zinc batteries, ACS Appl. Mater. Interfaces 12 (2020) 42763–42772.

[73] J.H. Zhou, F. Wu, Y. Mei, Y.T. Hao, L. Li, M. Xie, R.J. Chen, Establishing thermal infusion method for stable zinc metal anodes in aqueous zinc-ion batteries, Adv. Mater. 34 (2022) 2200782.

[74] P. Cao, X. Zhou, A. Wei, Q. Meng, H. Ye, W. Liu, J. Tang, J. Yang, Fast-charging and ultrahigh-capacity zinc metal anode for high-performance aqueous zinc-ion batteries, Adv. Funct. Mater. 31 (2021) 2100398.

[75] X. Xie, S. Liang, J. Gao, S. Guo, J. Guo, C. Wang, G. Xu, X. Wu, G. Chen, J. Zhou, Manipulating the ion-transfer kinetics and interface stability for high-performance zinc metal anodes, Energy Environ. Sci. 13 (2020) 503–510.

[76] M. Zhou, S. Guo, G. Fang, H. Sun, X. Cao, J. Zhou, A. Pan, S. Liang, Suppressing by-product via stratified adsorption effect to assist highly reversible zinc anode in aqueous electrolyte, J. Energy Chem. 55 (2021) 549–556.

[77] Y. Yang, C. Liu, Z. Lv, H. Yang, X. Cheng, S. Zhang, M. Ye, Y. Zhang, L. Chen, J. Zhao, C.C. Li, Redistributing Zn-ion flux by interlayer ion channels in Mg-Al layered double hydroxide-based artificial solid electrolyte interface for ultra-stable and dendrite-free Zn metal anodes, Energy Stor. Mater. 41 (2021) 230–239.

[78] L. Zhang, B. Zhang, T. Zhang, T. Li, T. Shi, W. Li, T. Shen, X. Huang, J. Xu, X. Zhang, Z. Wang, Y. Hou, Eliminating dendrites and side reactions via a multifunctional ZnSe protective layer toward advanced aqueous Zn metal batteries, Adv. Funct. Mater. 31 (2021) 2100186.

[79] H. Yan, S. Li, Y. Nan, S. Yang, B. Li, Ultrafast zinc-ion-conductor interface toward high-rate and stable zinc metal batteries, Adv. Energy Mater. 11 (2021) 2100186.

[80] Y. Yang, C. Liu, Z. Lv, H. Yang, Y. Zhang, M. Ye, L. Chen, J. Zhao, C.C. Li, Synergistic manipulation of Zn^{2+} ion flux and desolvation effect enabled by anodic growth of a 3D ZnF_2 matrix for long-lifespan and dendrite-free Zn metal anodes, Adv. Mater. 33 (2021) 2007388.

[81] P. Wang, S. Liang, C. Chen, X. Xie, J. Chen, Z. Liu, Y. Tang, B. Lu, J. Zhou, Spontaneous construction of nucleophilic carbonyl-containing interphase toward ultrastable zinc-metal anodes, Adv. Mater. 34 (2022) 2202733.

[82] F. Zhang, C. Wang, J. Pan, F. Tian, S. Zeng, J. Yang, Y. Qian, Polypyrrole-controlled plating/stripping for advanced zinc metal anodes, Mater. Today Energy 17 (2020) 100443.

[83] Z. Li, W. Deng, C. Li, W. Wang, Z. Zhou, Y. Li, X. Yuan, J. Hu, M. Zhang, J. Zhu, W. Tang, X. Wang, R. Li, Uniformizing the electric field distribution and ion migration during zinc plating/stripping via a binary polymer blend artificial interphase, J. Mater. Chem. A 8 (2020) 17725–17731.

[84] H. Wang, H. Li, Y. Tang, Z. Xu, K. Wang, Q. Li, B. He, Y. Liu, M. Ge, S. Chen, T. Hao, G. Xing, Y. Zhang, Stabilizing Zn anode interface by simultaneously manipulating the thermodynamics of Zn nucleation and overpotential of hydrogen evolution, Adv. Funct. Mater. (2022) 2207898.

[85] S.H. Park, S.Y. Byeon, J.-H. Park, C. Kim, Insight into the critical role of surface hydrophilicity for dendrite-free zinc metal anodes, ACS Energy Lett. 6 (2021) 3078–3085.

[86] P. He, J. Huang, Chemical passivation stabilizes Zn anode, Adv. Mater. 34 (2022) 2109872.

[87] Q. Zhang, J. Luan, X. Huang, Q. Wang, D. Sun, Y. Tang, X. Ji, H. Wang, Revealing the role of crystal orientation of protective layers for stable zinc anode, Nat. Commun. 11 (2020) 3961.

[88] L. Kang, M. Cui, F. Jiang, Y. Gao, H. Luo, J. Liu, W. Liang, C. Zhi, Nanoporous $CaCO_3$ coatings enabled uniform zn stripping/plating for long-life zinc rechargeable aqueous batteries, Adv. Energy Mater. 8 (2018) 1801090.

[89] J. Wang, Z. Cai, R. Xiao, Y. Ou, R. Zhan, Z. Yuan, Y. Sun, A chemically polished zinc metal electrode with a ridge-like structure for cycle-stable aqueous batteries, ACS Appl. Mater. Interfaces 12 (2020) 23028–23034.

[90] R. Xiao, Z. Cai, R. Zhan, J. Wang, Y. Ou, Z. Yuan, L. Wang, Z. Lu, Y. Sun, Localizing concentrated electrolyte in pore geometry for highly reversible aqueous Zn metal batteries, Chem. Eng. J. 420 (2021) 129642.

[91] Z. Cai, Y. Ou, B. Zhang, J. Wang, L. Fu, M. Wan, G. Li, W. Wang, L. Wang, J. Jiang, Z.W. Seh, E. Hu, X.-Q. Yang, Y. Cui, Y. Sun, A replacement reaction enabled interdigitated metal/solid electrolyte architecture for battery cycling at 20 mAcm^{-2} and 20 mAh cm^{-2}, J. Am. Chem. Soc. 143 (2021) 3143–3152.

[92] D. Wang, D. Lv, H. Peng, N. Wang, H. Liu, J. Yang, Y. Qian, Site-selective adsorption on ZnF_2/Ag coated Zn for advanced aqueous zinc–metal batteries at low temperature, Nano Lett. 22 (2022) 1750–1758.

[93] M. Kwon, J. Lee, S. Ko, G. Lim, S.-H. Yu, J. Hong, M. Lee, Stimulating Cu-Zn alloying for compact Zn metal growth towards high energy aqueous batteries and hybrid supercapacitors, Energy Environ. Sci. 15 (2022) 2889–2899.

[94] H. Peng, C. Liu, N. Wang, C. Wang, D. Wang, Y. Li, B. Chen, J. Yang, Y. Qian, Intercalation of organics into layered structures enables superior interface compatibility and fast charge diffusion for dendrite-free Zn anodes, Energy Environ. Sci. 15 (2022) 1682–1693.

[95] R. Xue, J. Kong, Y. Wu, Y. Wang, X. Kong, M. Gong, L. Zhang, X. Lin, D. Wang, Highly reversible zinc metal anodes enabled by a three-dimensional silver host for aqueous batteries, J. Mater. Chem. A 10 (2022) 10043–10050.

[96] J. Zhu, Z. Bie, X. Cai, Z. Jiao, Z. Wang, J. Tao, W. Song, H.J. Fan, A molecular-sieve electrolyte membrane enables separator-free zinc batteries with ultralong cycle life, Adv. Mater. 34 (2022) 2207209.

[97] Y. Ou, Z. Cai, J. Wang, R. Zhan, S. Liu, Z. Lu, Y. Sun, Reversible aqueous Zn battery anode enabled by a stable complexation adsorbent interface, EcoMat 4 (2022) e12167.

[98] J. Cao, D. Zhang, R. Chanajaree, Y. Yue, Z. Zeng, X. Zhang, J. Qin, Stabilizing zinc anode via a chelation and desolvation electrolyte additive, Adv. Powder Mater. 1 (2022) 100007.

[99] S.J. Zhang, J. Hao, D. Luo, P.F. Zhang, B. Zhang, K. Davey, Z. Lin, S.Z. Qiao, Dual-function electrolyte additive for highly reversible Zn anode, Adv. Energy Mater. 11 (2021) 2102010.

[100] X. Zeng, J. Mao, J. Hao, J. Liu, S. Liu, Z. Wang, Y. Wang, S. Zhang, T. Zheng, J. Liu, P. Rao, Z. Guo, Electrolyte design for in situ construction of highly Zn^{2+} -conductive solid electrolyte interphase to enable high-performance aqueous Zn-ion batteries under practical conditions, Adv. Mater. 33 (2021) 2007416.

[101] L. Cao, D. Li, T. Pollard, T. Deng, B. Zhang, C. Yang, L. Chen, J. Vatamanu, E. Hu, M.J. Hourwitz, L. Ma, M. Ding, Q. Li, S. Hou, K. Gaskell, J.T. Fourkas, X.Q. Yang, K. Xu, O. Borodin, C. Wang, Fluorinated interphase enables reversible aqueous zinc battery chemistries, Nat. Nanotechnol. 16 (2021) 902–910.

[102] Y. Zhong, Z. Cheng, H. Zhang, J. Li, D. Liu, Y. Liao, J. Meng, Y. Shen, Y. Huang, Monosodium glutamate, an effective electrolyte additive to enhance cycling performance of Zn anode in aqueous battery, Nano Energy 98 (2022) 107220.

[103] M. Yan, C. Xu, Y. Sun, H. Pan, H. Li, Manipulating Zn anode reactions through salt anion involving hydrogen bonding network in aqueous electrolytes with PEO additive, Nano Energy 82 (2021) 105739.

[104] P. Sun, L. Ma, W. Zhou, M. Qiu, Z. Wang, D. Chao, W. Mai, Simultaneous regulation on solvation shell and electrode interface for dendrite-free Zn ion batteries: achieved by a low-cost glucose additive, Angew. Chem. Int. Ed. 60 (2021) 18247–18255.

[105] Y.-P. Deng, R. Liang, G. Jiang, Y. Jiang, A. Yu, Z. Chen, The current state of aqueous Zn-based rechargeable batteries, ACS Energy Lett. 5 (2020) 1665–1675.

[106] S.Y. Cai, X.Y. Chu, C. Liu, H.W. Lai, H. Chen, Y.Q. Jiang, F. Guo, Z.K. Xu, C.S. Wang, C. Gao, Water-salt oligomers enable supersoluble electrolytes for high-performance aqueous batteries, Adv. Mater. 33 (2021) 2007470.

[107] S. Liu, J. Mao, W.K. Pang, J. Vongsvivut, X. Zeng, L. Thomsen, Y. Wang, J. Liu, D. Li, Z. Guo, Tuning the electrolyte solvation structure to suppress cathode dissolution, water reactivity, and Zn dendrite growth in zinc-ion batteries, Adv. Funct. Mater. 31 (2021) 2104281.

[108] Q. Nian, X. Zhang, Y. Feng, S. Liu, T. Sun, S. Zheng, X. Ren, Z. Tao, D. Zhang, J. Chen, Designing electrolyte structure to suppress hydrogen evolution reaction in aqueous batteries, ACS Energy Lett. 6 (2021) 2174–2180.

[109] W. Yang, X. Du, J. Zhao, Z. Chen, J. Li, J. Xie, Y. Zhang, Z. Cui, Q. Kong, Z. Zhao, C. Wang, Q. Zhang, G. Cui, Hydrated eutectic electrolytes with ligand-oriented solvation shells for long-cycling zinc-organic batteries, Joule 4 (2020) 1557–1574.

[110] J. Zhao, J. Zhang, W. Yang, B. Chen, Z. Zhao, H. Qiu, S. Dong, X. Zhou, G. Cui, L. Chen, Water-in-deep eutectic solvent" electrolytes enable zinc metal anodes for rechargeable aqueous batteries, Nano Energy 57 (2019) 625–634.

[111] H. Qiu, X. Du, J. Zhao, Y. Wang, J. Ju, Z. Chen, Z. Hu, D. Yan, X. Zhou, G. Cui, Zinc anode-compatible in-situ solid electrolyte interphase via cation solvation modulation, Nat. Commun. 10 (2019) 5374.

[112] R. Zhao, H. Wang, H. Du, Y. Yang, Z. Gao, L. Qie, Y. Huang, Lanthanum nitrate as aqueous electrolyte additive for favourable zinc metal electrodeposition, Nat. Commun. 13 (2022) 3252.

[113] L. Zhou, F. Wang, F. Yang, X. Liu, Y. Yu, D. Zheng, X. Lu, Unshared pair electrons of zincophilic lewis base enable long-life Zn anodes under “three high” conditions, Angew. Chem. Int. Ed. 61 (2022) e202208051.

[114] Y. Shang, P. Kumar, T. Musso, U. Mittal, Q. Du, X. Liang, D. Kundu, Long-life Zn anode enabled by low volume concentration of a benign electrolyte additive, Adv. Funct. Mater. 32 (2022) 2200606.

[115] Z. Zhu, Y. Geng, L. Miao, Z. Yan, W. Xin, L. Zhang, H. Peng, J. Li, Super-zincophilic additive induced interphase modulation enables long-life Zn anode under high current density and areal capacity, J. Mater. Chem. A 10 (2022) 10132–10138.